Uncertainty quantification for hybrid random logistic models with harvesting via density functions

J.-C. Cortés[a,*], A. Moscardó-García[a], R.-J. Villanueva[a]

[a] *Instituto Universitario de Matemática Multidisciplinar, Universitat Politècnica de València, Camino de Vera s/n, 46022, Valencia, Spain*

Abstract

The so-called logistic model with harvesting, $p'(t) = rp(t)\left(1 - \frac{p(t)}{K}\right) - c(t)p(t)$, $p(t_0) = p_0$, is a classical ecological model that has been extensively studied and applied in the deterministic setting. It has also been studied, to some extent, in the stochastic framework using the Itô Calculus by formulating a Stochastic Differential Equation whose uncertainty is driven by the Gaussian white noise. In this paper, we present a new approach, based on the so-called theory of Random Differential Equations, that permits treating all model parameters as a random vector with an arbitrary join probability distribution (so, not just Gaussian). We take extensive advantage of the Random Variable Transformation method to probabilistically solve the full randomized version of the above logistic model with harvesting. It is done by exactly computing the first probability density function of the solution assuming that all model parameters are continuous random variables with an arbitrary join probability density function. The probabilistic solution is obtained in three relevant scenarios where the harvesting or influence function is mathematically described by discontinuous parametric stochastic processes having a biological meaning. The probabilistic analysis also includes the computation of the probability density function of the nontrivial equilibrium state, as well as the probability that stability is reached. All these results are new and extend their deterministic counterpart under very general assumptions. The theoretical findings are illustrated via two numerical examples. Finally, we show a detailed example where results are applied to describe the dynamics of stock of fishes over time using real data.

Keywords: hybrid random differential equation, uncertainty quantification, first probability density function, real-world application, random variable transformation technique

1. Introduction and preliminaries

The mathematical modelling of population growth has attracted the attention of numerous studies starting from the seminal paper by T.R. Malthus [1, 2]. It is well-known that this model is formulated via the following linear differential equation, $p'(t) = rp(t)$, where $p(t)$ denotes the population size at the time instant $t > 0$ and r represents the *per capita* growth rate. Despite its

[*] Corresponding author

Email addresses: jccortes@imm.upv.es (J.-C. Cortés), amosgar@alumni.uv.es (A. Moscardó-García), rjvillan@imm.upv.es (R.-J. Villanueva)

simplicity and strong criticism about it [3], the Malthusian model seems to be fairly adequate to explain the first growth stage of many biological populations and, in general, of growth processes, for which a rapid exponential growth ($r >> 0$) is observed, namely $p(t) = p_0 e^{rt}$, being p_0 the size of the initial population [4, 5]. The investigation of Malthusian model still continues attracting researchers via new and appealing analysis where uncertainties play a key role [6, 7, 8, 9, 10]. The main flaw of Malthusian model is that, when $r > 0$, it predicts infinite growth in the long-term despite resources (like, for example, food in the biological context) are always limited. Motivated by this drawback, P.F. Verhulst proposed the celebrated logistic model [11, 12], formulated by the following initial value problem (IVP)

$$p'(t) = rp(t)\left(1 - \frac{p(t)}{K}\right), \qquad p(t_0) = p_0, \tag{1}$$

where $K > 0$ represents the carrying capacity. The logistic model can be regarded as a generalization of the Malthusian one whose *per capita* growth rate, say $\hat{r}$, is not constant but depending on both the population size at the time instant t, $p(t)$, and the carrying capacity, K, i.e. $p'(t) = \hat{r}p(t)$ where $\hat{r} = r\left(1 - \frac{p(t)}{K}\right)$. It is well-known that the solution of model (1) is given by $p(t) = \frac{p_0 K e^{r(t-t_0)}}{K + p_0\left(e^{r(t-t_0)} - 1\right)}$ and that $p(t) \to K$ as $t \to \infty$, provided $r > 0$, regardless the initial condition p_0.

The logistic model, and some generalizations of it, have been extensively investigated and applied in different contexts. In [13], one obtains the explicit solution of a class of non-autonomous logistic models whose carrying capacity is time-dependent, $K(t)$, and defined via different functional forms in order to better describe changes in the environment. In [14], one investigates the case where $K(t)$ depends on the population at an earlier time, capturing a delay in the way the population modifies its environment. This leads to the logistic delay differential equation. In [15] one specifically deals with the following generalization of model (1), usually referred to as the logistic model with capture,

$$p'(t) = rp(t)\left(1 - \frac{p(t)}{K}\right) - c(t)p(t), \qquad p(t_0) = p_0. \tag{2}$$

The term $c(t)p(t)$ is called the harvesting or influence function and the factor $c(t)$ is the harvesting intensity coefficient.

The study of the logistic model with uncertainties has been conducted mainly using two different approaches, namely, via stochastic differential equations (SDEs) and via random differential equations (RDEs).

On the one hand, SDEs are driven by the Wiener stochastic process, which is Gaussian and with nowhere differentiable trajectories. The rigorous treatment of SDEs requires the application of Itô or Stratonovic stochastic calculus [16, 17, 18]. In the extant literature, the study of the logistic SDE has included the asymptotic analysis of the equilibrium state [19, 20], the computation of main statistical quantities of interest (distribution of the solution, the mean passage time, the distribution of hitting times, etc.) [21], the numerical approximation of its solution by discretizations [22], the computation of time-dependent densities [23], etc. It is also important to point out that different variations of the logistic SDE have been proposed using distributed or infinite delays [24, 25], impulsive control [26, 27] and other formulations.

On the other hand, in the setting of RDEs, uncertainties are directly assigned to model inputs (initial/boundary conditions, forcing term and/or coefficients) via random variables or stochastic processes whose sample behaviour is fairly regular (e.g., continuity) [28, 29]. This approach provides more flexibility when assigning probability distributions to model inputs since apart from the Gaussian pattern other relevant probability distributions are also allowed (binomial, Poisson, Beta, Exponential, etc.) [29]. This key fact makes RDEs particularly attractive for modelling purposes. Results about RDEs are scarcer than the ones for SDEs. Some interesting contributions have been recently obtained for the logistic RDE [30, 31, 32, 33]. In these contributions the classical or standard randomized logistic model (obtained when $c(t) = 0$ in (2)) is studied via the calculation of the probability density function (p.d.f.) of the solution, in two main cases, first when the carrying capacity is a random variable [30, 31], and secondly, when it is a stochastic process [32, 33].

The aim of this paper is to study a full randomized version of model (2) by assuming that the harvesting coefficient $c(t)$ is a parametric stochastic process with jumps (discontinuous) at specific time instants, say, t_i. For the sake of generality, in our analysis, we will assume that the size of jumps at t_i, randomly fluctuates, and it will be represented by a random variable, c_i, that determines the harvesting intensity. Then, this model is defined by a hybrid RDE. As it shall be later indicated, we will consider different functional forms of $c(t)$ that reasonably represent the way capture (or harvesting) is made. To the best of our knowledge this randomized model has not been studied yet, and our analysis can be regarded as complementing the previous aforementioned studies for the standard logistic RDE. Indeed, our main goal in this paper is to determine, under very general hypotheses, the first probability density function (1-p.d.f.) of the solution stochastic process [34, 28], as well as to study, from a probabilistic point of view, the stability of the non-trivial solution of model (2). To conduct our analysis the so-called Random Variable Transformation (RVT) method will be extensively applied throughout the paper. The RVT technique is a powerful tool that, in its continuous formulation, permits computing the p.d.f. of an absolutely continuous random vector, which results from mapping another absolutely continuous random vector whose p.d.f. is known [35], [36, Th. 2.1.5]. It is important to point out that computing the 1-p.d.f. of a stochastic process is a major goal, since by integrating the 1-p.d.f. one can calculate every one-dimensional moments of the stochastic process, provided they exist. In particular, the mean and the variance as well as the probability that the process lies within a specific interval of interest can be obtained by the 1-p.d.f. This latter information can be of paramount usefulness in practice to account, for example, the probability that the number of individuals of an endangered species varies within a critical range.

For the sake of generality, hereinafter we will assume that all model inputs in the IVP (2), i.e., p_0, r, K, c are positive absolutely continuous random variables defined in a common complete probability space $(\Omega, \mathcal{F}, \mathbb{P})$ with a joint p.d.f., $f_{p_0,r,K,c} := f_{p_0,r,K,c}(p_0, r, K, c)$. As usual, we will omit the ω-notation when convenient, so, for example, we will denote p_0 or $p_0(\omega)$, indistinctly, and the same can be said for the rest of random variables or stochastic processes throughout the paper. To keep our mathematical development as general as possible, observe that we do not assume that model inputs are independent random variables. In that particular case, $f_{p_0,r,K,c} = f_{p_0} f_r f_K f_c$ being $f_{p_0} := f_{p_0}(p_0)$, $f_r := f_r(r)$, $f_K := f_K(K)$ and $f_c := f_c(c)$ the marginal p.d.f.'s of p_0, r, K and c, respectively. Since independence hypothesis is not only usual when performing theoretical stochastic analysis but also realistic in many real scenarios, in our subsequent analysis we will specialize some of our findings to this relevant scenario.

The paper is organized as follows. In Section 2, we will give an explicit expression for the 1-p.d.f. of the solution stochastic process, $p(t)$, of the randomized logistic model (2), in three relevant case studies with respect to the functional form of the harvesting term. In Section 3, we determine the p.d.f. of the non-trivial equilibrium state as well as the probability of reaching stability. In Section 4, the theoretical findings established in the previous sections are illustrated by means of several numerical examples that cover all the case studies presented in Section 2 as well as the random stability analysis. In Section 5, we show how the theoretical results can be applied to perform an Uncertainty Quantification analysis for the hybrid logistic model (2) using real-world data. Conclusions are drawn in Section 6.

2. Stochastic analysis via the first probability density function

In this section we analyze a randomized version of model (2). According to [15], the analytical solution of this model is given by

$$p(t) = \frac{p_0 K q(t)}{K + r p_0 \displaystyle\int_{t_0}^{t} q(z)\,\mathrm{d}z}, \qquad q(z) = \exp\left(\int_{t_0}^{z} (r - c(\tau))\,\mathrm{d}\tau\right). \tag{3}$$

It is interesting to remark that in the particular case that $r - c(t) = b$, the classical Verhulst model is obtained with the following identification of parameters: growth rate b, initial condition p_0 and carrying capacity Kb/r.

Now, we will determine the 1-p.d.f., $f_{p(t)} := f_{p(t)}(p)$, of $p = p(t)$ given in (3), regarded as a parametric stochastic process that depends on the absolutely continuous random variables p_0, r, K and c, whose joint p.d.f. is denoted by $f_{p_0,r,K,c}$. To this end, it is convenient to denote

$$h(t) = \int_{t_0}^{t} q(z)\,\mathrm{d}z, \quad t \geq t_0. \tag{4}$$

Then

$$p(t) = \frac{p_0\, K\, q(t)}{K + r\, p_0\, h(t)}. \tag{5}$$

Let fix $t \geq t_0$ and then we apply the RVT method using the following mapping,

$$(p_0, r, K, c) \longmapsto (X, Y, p, Z) = \left(p_0, r, \frac{p_0\, K\, q(t)}{K + r\, p_0\, h(t)}, c\right). \tag{6}$$

This mapping is invertible and its inverse is defined by

$$(X, Y, p, Z) \longmapsto (p_0, r, K, c) = \left(X, Y, \frac{Y\, X\, p\, h(t)}{X\, q(t) - p}, Z\right). \tag{7}$$

The 1-p.d.f, $f_{p(t)}$, can be calculated in terms of the p.d.f., $f_{X,Y,p,Z} := f_{X,Y,p,Z}(X, Y, p, Z)$, of the random vector (X, Y, p, Z) via the following marginalization

$$f_{p(t)}(p) = \int_{\mathcal{D}(X,Y,Z)} f_{X,Y,p,Z}(X, Y, p, Z)\,\mathrm{d}X\,\mathrm{d}Y\,\mathrm{d}Z,$$

where $\mathcal{D}(X, Y, Z)$ denotes the domain of the random vector (X, Y, Z). Finally, let us observe that $f_{p(t)}$ can be directly expressed in terms of data by calculating the p.d.f., $f_{X,Y,p,Z}$, in terms of $f_{p_0,r,K,c}$ by means of the RVT method

$$f_{p(t)}(p) = \int_{\mathcal{D}(p_0,r,c)} f_{p_0,r,K,c}\left(p_0, r, \frac{r\, p_0\, p\, h(t)}{p_0\, q(t) - p}, c\right) |J(X, Y, p, Z)|\,\mathrm{d}p_0\,\mathrm{d}r\,\mathrm{d}c, \tag{8}$$

where $|J(X, Y, p, Z)|$ represents the absolute value of the Jacobian matrix determinant of the mapping given by (7)

$$J(X, Y, p, Z) = \det \begin{pmatrix} \frac{\partial p_0}{\partial X} & \frac{\partial p_0}{\partial Y} & \frac{\partial p_0}{\partial p} & \frac{\partial p_0}{\partial Z} \\ \frac{\partial r}{\partial X} & \frac{\partial r}{\partial Y} & \frac{\partial r}{\partial p} & \frac{\partial r}{\partial Z} \\ \frac{\partial K}{\partial X} & \frac{\partial K}{\partial Y} & \frac{\partial K}{\partial p} & \frac{\partial K}{\partial Z} \\ \frac{\partial c}{\partial X} & \frac{\partial c}{\partial Y} & \frac{\partial c}{\partial p} & \frac{\partial c}{\partial Z} \end{pmatrix} = \frac{\partial K}{\partial p} = \frac{r\, p_0^2\, q(t)\, h(t)}{(p_0\, q(t) - p)^2}.$$

Notice that in the last step we have used (6) and (7). Since $q(t) > 0$ (see (3)), hence $h(t) > 0$ too (see (4)), and also p_0 and r are positive random variables, then $|J(X, Y, p, Z)| = J(X, Y, p, Z) > 0$ and by substituting the value of $J(X, Y, p, Z)$ into (8), one obtains the following explicit expression for the 1-p.d.f. of the solution stochastic process of model (2),

$$f_{p(t)}(p) = \int_{\mathcal{D}(p_0,r,c)} f_{p_0,r,K,c}\left(p_0, r, \frac{r\, p_0\, p\, h(t)}{p_0\, q(t) - p}, c\right) \frac{r\, p_0^2\, q(t)\, h(t)}{(p_0\, q(t) - p)^2}\, \mathrm{d}p_0\, \mathrm{d}r\, \mathrm{d}c. \tag{9}$$

In the following remarks, we give alternative expressions for $f_{p(t)}(p)$ in relevant particular cases where independence about some model inputs is assumed.

Remark 1. In the case that p_0, r, K and c are independent random variables, expression (9) writes

$$f_{p(t)}(p) = \int_{\mathcal{D}(c)} \int_{\mathcal{D}(r)} \int_{\mathcal{D}(p_0)} f_{p_0}(p_0) f_r(r) f_K\left(\frac{r\, p_0\, p\, h(t)}{p_0\, q(t) - p}\right) f_c(c)\, \frac{r\, p_0^2\, q(t)\, h(t)}{(p_0\, q(t) - p)^2}\, \mathrm{d}p_0\, \mathrm{d}r\, \mathrm{d}c. \tag{10}$$

Remark 2. The independence hypothesis assumed in Remark 1 can be relaxed so that $f_{p(t)}$ can be expressed as an expectation. For example, if the random vector (p_0, r, c) and the random variable K are independent, then

$$\begin{aligned} f_{p(t)}(p) &= \int_{\mathcal{D}(p_0,r,c)} f_{p_0,r,c}(p_0, r, c) f_K\left(\frac{r\, p_0\, p(t)\, h(t)}{p_0\, q(t) - p(t)}\right) \frac{r\, p_0^2\, q(t)\, h(t)}{(p_0\, q(t) - p(t))^2}\, \mathrm{d}p_0\, \mathrm{d}r\, \mathrm{d}c \\ &= \mathbb{E}_{p_0,r,c}\left[f_K\left(\frac{r\, p_0\, p(t)\, h(t)}{p_0\, q(t) - p}\right) \frac{r\, p_0^2\, q(t)\, h(t)}{(p_0\, q(t) - p(t))^2} \right], \end{aligned} \tag{11}$$

where $\mathbb{E}_{p_0,r,c}[\ ]$ stands for the expectation with respect to the random vector (p_0, r, c). This expression is particularly useful to compute the 1-p.d.f. $f_{p(t)}$ via Monte Carlo simulations [37] and it will be used in the numerical examples exhibited in Section 4.

Remark 3. It is important to point out that the calculation of the 1-p.d.f. has been based on the definition of mapping (6), but other mappings can also be appropriate to achieve the goal. The key points that make our mapping success are that the solution stochastic process can be obtained from the mapping (in our case is exactly its third component), and that it has an inverse mapping, which is also computable. For example, the following mapping can alternatively be considered to determine the 1-p.d.f.

$$(p_0, r, K, c) \longmapsto (p, X, Y, Z) = \left(\frac{p_0\, K\, q(t)}{K + r\, p_0\, h(t)}, r, K, c\right). \tag{12}$$

Notice that in the definition of both mappings, (6) and (12), we define them through the identity transformation of the random model parameters, except for one of the components that is just the solution itself. Notice that the corresponding inverse mappings can be easily computed. Finally, notice that the final expression that we would obtain using the mapping (12) is not the same as (9), but equivalent.

In the rest of this section, we will determine the 1-p.d.f., $f_{p(t)}$, of the solution stochastic process, $p(t)$, of model (2) in several particular cases with regard to the specific form of the harvesting intensity coefficient $c(t)$. With this aim, and for the sake of clarity in the presentation, our subsequent analysis is divided into three subsections where different forms for $c(t)$ are considered. Each one of them corresponds to distinct types of harvesting, which can be biologically interpreted. To carry out our analysis, it is important to observe that, according to (5), $p(t)$ depends on $c(t)$ via $q(t)$ and $h(t)$ (see (3) and (4)). Therefore, in each subsection we will only concentrate on determining explicit expressions for $q(t)$ and $h(t)$ in each case. Our findings extend to the stochastic scenario the deterministic results presented in [15] and permit considering more general forms for the harvesting intensity coefficient $c(t)$.

2.1. *Case I: A perpetual capture with random intensity is applied*

In this first case, we assume that the parametric stochastic process $c(t)$ is defined via the Heaviside step function (also termed unit step function), $\theta(\cdot)$, [38]

$$c(t) = c\theta(t - t_1) = \begin{cases} 0, & t \le t_1, \\ c, & t > t_1, \end{cases} \tag{13}$$

where, in our context $t_1 > t_0$ is fixed and $c = c(\omega)$, $\omega \in \Omega$, is a random variable. This case can be biologically interpreted as that a perpetual capture with a random intensity, modelled via c, is made from the time instant t_1. Notice that in practice, the value of c may fluctuate, for example due to environment factors, so it is better described by means of a random quantity. Note that in the solution given by (3), $c(t)$ only appears via the term $q(z)$ and its integral $h(t)$ (see (4)). So, according to (3) and (13), for $z \le t_1$, one gets

$$q(z) = \exp\left(\int_{t_0}^{z} r \, \mathrm{d}\tau\right) = \mathrm{e}^{r(z-t_0)},$$

and for $z > t_1$

$$q(z) = \exp\left(\int_{t_0}^{t_1} r \, \mathrm{d}\tau + \int_{t_1}^{z} r - c \, \mathrm{d}\tau\right) = \mathrm{e}^{r(z-t_0)-c(z-t_1)}.$$

Therefore,

$$q(z) = \begin{cases} \mathrm{e}^{r(z-t_0)}, & z \le t_1, \\ \mathrm{e}^{r(z-t_0)-c(z-t_1)}, & z > t_1. \end{cases} \tag{14}$$

Then, according to (4), for $t \le t_1$, one gets

$$h(t) = \int_{t_0}^{t} \mathrm{e}^{r(z-t_0)} \, \mathrm{d}z = \frac{1}{r}\left(\mathrm{e}^{r(t-t_0)} - 1\right)$$

and, for $t > t_1$,

$$\begin{aligned} h(t) &= \int_{t_0}^{t_1} \mathrm{e}^{r(z-t_0)} \, \mathrm{d}z + \int_{t_1}^{t} \mathrm{e}^{r(z-t_0)-c(z-t_1)} \, \mathrm{d}z \\ &= \frac{1}{r}\left(\mathrm{e}^{r(t_1-t_0)} - 1\right) + \frac{1}{r-c}\left(\mathrm{e}^{r(t-t_0)-c(t-t_1)} - \mathrm{e}^{r(t_1-t_0)}\right). \end{aligned}$$

Summarizing,

$$h(t)=\begin{cases}\dfrac{1}{r}\left(\mathrm{e}^{r(t-t_0)}-1\right), & t\le t_1,\\[2ex] \dfrac{1}{r}\left(\mathrm{e}^{r(t_1-t_0)}-1\right)+\dfrac{1}{r-c}\left(\mathrm{e}^{r(t-t_0)-c(t-t_1)}-\mathrm{e}^{r(t_1-t_0)}\right), & t>t_1.\end{cases}\tag{15}$$

Notice that in this case the 1-p.d.f., $f_{p(t)}$, given by (9), is defined in two pieces, for $t_0 \le t \le t_1$ and for $t > t_1$, according to piecewise functions $q(t)$ and $h(t)$, given in (14) and (15), respectively.

2.2. *Case II: Several capture periods with different random intensities are applied*

In the foregoing Case I, we have assumed that a single perennial capture is made with a uncertain fluctuating intensity described by the random variable $c = c(\omega)$, $\omega \in \Omega$. However, it seems more realistic that such harvesting period only lasts for a finite period, say $]t_1, t_2]$, being $t_1 > t_0$. This can be mathematically expressed by the Heaviside function as

$$c(t)=c\left[\theta(t-t_1)-\theta(t-t_2)\right]=\begin{cases}0, & t\le t_1,\\ c, & t_1<t\le t_2,\\ 0, & t>t_2.\end{cases}\tag{16}$$

This situation happens in different biological scenarios such as the fishing or hunting periods practiced by humans, whose dates are usually regulated by administrations or, in the case of wild predators that hunt preys, only during specific periods.

As it has been previously indicated, to determine the 1-p.d.f., $f_{p(t)}$, of the solution stochastic process it is enough to obtain the functions $q(t)$ and $h(t)$ defined in (3) and (4), respectively. To facilitate the presentation of calculations of these two functions, we will first analyze the simplest case, when $c(t)$ is defined by (16), and afterwards, we will generalize the results for the case that a finite number of harvesting, each one with a different duration and intensity, is made. In contrast to Case I, the computations will be now directly presented.

So, let us assume that $c(t)$ is given by (16). Then, following a similar reasoning as in Case I, $q(z)$ and $h(t)$ can be calculated. For $q(z)$ one gets

$$q(z)=\begin{cases}\mathrm{e}^{r(z-t_0)}, & z\le t_1,\\ \mathrm{e}^{(ct_1-rt_0)-(c-r)z}, & t_1<z\le t_2,\\ \mathrm{e}^{r(z-t_0)-c(t_2-t_1)}, & z>t_2.\end{cases}$$

While for $h(t)$, one obtains

$$h(t)=\begin{cases}\dfrac{1}{r}\left(\mathrm{e}^{r(t-t_0)}-1\right), & z\le t_1,\\[2ex] \dfrac{1}{r}\left(A_1-1\right)+\dfrac{1}{r-c}\left(D\mathrm{e}^{-(c-r)t}-A_1\right), & t_1<z\le t_2,\\[2ex] \dfrac{1}{r}\left(A_1-1\right)+\dfrac{1}{r-c}\left(D\mathrm{e}^{-(c-r)t}-A_1\right)+\dfrac{1}{r}B\left(\mathrm{e}^{r(t-t_0)}-A_2\right), & z>t_2.\end{cases}$$

These results have been calculated by computing the following integrals. For $t \le t_1$, $h(t) = \int_{t_0}^{t} \mathrm{e}^{r(z-t_0)}\,\mathrm{d}z$. For $t_1 < t \le t_2$, $h(t) = \int_{t_0}^{t_1} \mathrm{e}^{r(z-t_0)}\,\mathrm{d}z + \int_{t_1}^{t} D\mathrm{e}^{-(c-r)z}\,\mathrm{d}z$ being $D = \mathrm{e}^{ct_1-rt_0}$. And for

$t > t_2$, $h(t) = \int_{t_0}^{t_1} \mathrm{e}^{r(z-t_0)}\,\mathrm{d}z + \int_{t_1}^{t_2} D\mathrm{e}^{-(c-r)z}\,\mathrm{d}z + \int_{t_2}^{t} B\mathrm{e}^{r(z-t_0)}\,\mathrm{d}z$ being $B = \mathrm{e}^{-c(t_2-t_1)}$. To compact the notation with the general case that will be presented down below, we have also introduced the following notation, $A_1 = \mathrm{e}^{r(t_1-t_0)}$ and $A_2 = \mathrm{e}^{r(t_2-t_0)}$.

The foregoing scenario can be generalized in order to account for several captures made during more periods with different duration and applying a different fluctuating (uncertain) intensity within each one of these periods. With this aim, we will assume that the harvesting function is of the form

$$c(t) = \sum_{i=1}^{n-1} c_i \left[\theta(t-t_i) - \theta(t-t_{i+1})\right],$$

where $c_i = c_i(\omega)$, $\omega \in \Omega$, and $t_1 < t_2 < \cdots < t_{n-1} < t_n$, so now n periods are considered. This function is defined in order to describe fishing or hunting activities when captures are regulated depending on the population size or allowed during certain periods of the year. Assuming this particular function $c(t)$, the obtained expressions for $q(z)$ and $h(t)$ are

$$q(z) = \begin{cases} \mathrm{e}^{r(z-t_0)}, & z \le t_1, \\ \mathrm{e}^{r(z-t_0)-\sum_{i=1}^{k-1} c_i(t_{i+1}-t_i)-c_k(z-t_k)}, & t_k < z \le t_{k+1}, \quad k \in \{1,\ldots,n-1\}, \\ \mathrm{e}^{r(z-t_0)-\sum_{i=1}^{n-1} c_i(t_{i+1}-t_i)}, & z > t_n. \end{cases} \tag{17}$$

Then, for $t \le t_1$, $h(t)$ can be written as

$$h(t) = \frac{1}{r}\left(\mathrm{e}^{r(t-t_0)} - 1\right). \tag{18}$$

In the case that $t_k < t \le t_{k+1}$ for $k \in \{1,\ldots,n-1\}$, we first introduce the following notation

$$D_1 = \mathrm{e}^{c_1 t_1 - r t_0}, \quad B_i = \mathrm{e}^{-c_i(t_{i+1}-t_i)}, \quad A_i = \mathrm{e}^{r(t_i-t_0)}, \quad i \in \{1,2,\ldots,n\},$$

to simplify the subsequent expressions. After some technical computations, one obtains

$$\begin{aligned} h(t) &= \frac{1}{r}(A_1 - 1) + \frac{1}{r-c_1}\left(D_1\mathrm{e}^{-(c_1-r)t} - A_1\right) \\ &\quad + \sum_{i=2}^{k} \frac{1}{r-c_i} B_1 \cdots B_{i-1}\left(\mathrm{e}^{r(t-t_0)-c_i(t-t_0)} - A_i\right). \end{aligned} \tag{19}$$

Finally, for $t > t_n$,

$$\begin{aligned} h(t) &= \frac{1}{r}(A_1 - 1) + \frac{1}{r-c_1}\left(D_1\mathrm{e}^{-(c_1-r)t_n} - A_1\right) \\ &\quad + \sum_{i=2}^{n} \frac{1}{r-c_i} B_1 \cdots B_{i-1}\left(\mathrm{e}^{r(t_n-t_0)-c_i(t_n-t_0)} - A_i\right) \\ &\quad + \frac{1}{r} B_1 \cdots B_n\left(\mathrm{e}^{r(t-t_0)} - A_n\right). \end{aligned} \tag{20}$$

As a result, in this case the 1-p.d.f., $f_{p(t)}$, given by (9), is defined by $n+1$ pieces, $t_0 < t \le t_1$, $t_1 < t \le t_2$, ..., $t_{n-1} < t \le t_n$ and $t > t_n$, according to the piecewise functions $q(t)$ and $h(t)$, given in (17) and (18)–(20), respectively.

2.3. Case III: Punctual captures are applied

Finally, we analyze the case that only punctual captures are made, i.e. the duration of captures is negligible when compared with the total time of growth. In this case, the harvesting function can be modelled using the Dirac delta function [38]. As in the Case II, we will first present the results for the case that a punctual capture takes place at certain time, say t_1, with a fluctuating intensity, $c = c(\omega)$, $\omega \in \Omega$, i.e., we will assume that $c(t) = c\delta(t - t_1)$, being $\delta(\cdot)$ the Dirac delta function, and later on, we will consider a generalization of this previous situation. In the former case, applying the definition of $q(z)$, one obtains

$$q(z) = \exp\left(\int_{t_0}^{z} (r - c\delta(\tau - t_1))\,\mathrm{d}\tau\right) = \exp\left(r(z - t_0) - \int_{t_0}^{z} c\,\delta(\tau - t_1)\,\mathrm{d}\tau\right). \tag{21}$$

Using the following property of Dirac delta function [39],

$$\int_a^b f(\tau)\delta(\tau - t)\,\mathrm{d}\tau = \begin{cases} f(t), & a < \tau < b, \\ 0, & \text{otherwise}, \end{cases}$$

expression (21) can be simplified in terms of Heaviside function, $\theta(\cdot)$,

$$q(z) = \mathrm{e}^{r(z-t_0)-c\theta(z-t_1)} = \begin{cases} \mathrm{e}^{r(z-t_0)}, & z \leq t_1, \\ \mathrm{e}^{r(z-t_0)-c}, & z > t_1. \end{cases} \tag{22}$$

While, using the definition of $h(t)$ given in (4) and notation from the previous case, $A_i = \mathrm{e}^{r(t_i-t_0)}$, one obtains

$$h(t) = \begin{cases} \displaystyle\int_{t_0}^{t} \mathrm{e}^{r(z-t_0)}\,\mathrm{d}z = \frac{1}{r}\left(\mathrm{e}^{r(t-t_0)} - 1\right), & t \leq t_1, \\[2ex] \displaystyle\int_{t_0}^{t} \mathrm{e}^{r(z-t_0)-c}\,\mathrm{d}z = \frac{1}{r}(A_1 - 1) + \frac{\mathrm{e}^{-c}}{r}\left(\mathrm{e}^{r(t-t_0)} - A_1\right), & t > t_1. \end{cases} \tag{23}$$

Therefore, the 1-p.d.f., $f_{p(t)}$, given by (9), is defined in two pieces, $t_0 < t \leq t_1$ and $t > t_1$, according to the piecewise functions $q(t)$ and $h(t)$, given in (22) and (23), respectively.

Now, we assume that punctual captures take place at different time instants, t_i, having each one of them distinct random intensities, $c_i = c_i(\omega)$, $\omega \in \Omega$. This situation is modelled by means of the following harvesting function, $c(t) = \sum_{i=1}^{N} c_i\delta(t - t_i)$, $N = 1, 2, \ldots$. Then, the following expressions for $q(z)$ and $h(t)$ respectively are obtained

$$q(z) = \begin{cases} \mathrm{e}^{r(z-t_0)}, & z \leq t_1, \\ \mathrm{e}^{r(z-t_0)-\sum_{i=1}^{n} c_i}, & t_n < z \leq t_{n+1},\ n = 1, \ldots, N-1, \\ \mathrm{e}^{r(z-t_0)-\sum_{i=1}^{N} c_i}, & z > t_N, \end{cases} \tag{24}$$

and

$$h(t) = \begin{cases} \frac{1}{r}\left(\mathrm{e}^{r(t-t_0)} - 1\right), & z \leq t_1, \\[2ex] \frac{1}{r}(A_1 - 1) + \frac{1}{r}\sum_{j=1}^{n-1} \mathrm{e}^{-\sum_{i=1}^{j} c_i}\left(A_{j+1} - A_j\right) + \frac{\mathrm{e}^{-\sum_{i=1}^{n} c_i}}{r}\left(\mathrm{e}^{r(t-t_0)} - A_n\right), & t_n < z \leq t_{n+1},\ n = 1, \ldots, N-1, \\[2ex] \frac{1}{r}(A_1 - 1) + \frac{1}{r}\sum_{j=1}^{N-1} \mathrm{e}^{-\sum_{i=1}^{j} c_i}\left(A_{j+1} - A_j\right) + \frac{\mathrm{e}^{-\sum_{i=1}^{N} c_i}}{r}\left(\mathrm{e}^{r(t-t_0)} - A_N\right), & z > t_N. \end{cases} \tag{25}$$

The above results are easily adapted when $N = +\infty$, i.e., there are infinite punctual captures.

Similarly as in the second part of Case II, the 1-p.d.f., $f_{p(t)}$, given by (9), is defined in pieces, according to the piecewise functions $q(t)$ and $h(t)$, given in (24) and (25), respectively.

3. Probabilistic stability analysis

The aim of this section is to study, from a probabilistic standpoint, the stability of the randomized logistic model with capture, formulated by (2) in the case that the harvesting intensity coefficient, $c(t)$, becomes a random variable for t large enough, i.e. when $c(t) = c(t;\omega) = \hat{c}(\omega)$, $\omega \in \Omega$ for all $t \geq \hat{t}$. Observe that this happens in the three cases analyzed in the previous section. Indeed, in Case I: $\hat{c}(\omega) = c(\omega)$ and $\hat{t} = t_1$; in Case II: $\hat{c}(\omega) = 0$ and $\hat{t} = t_n$; in Case III: $\hat{c}(\omega) = 0$ and $\hat{t} > t_N$ with N finite. In these two latter scenarios, the equilibrium state will intuitively match the one corresponding to the classical logistic model (i.e., with no capture).
Down below, our analysis will focus on computing the p.d.f. of the equilibrium or steady state, which is also a random variable, as well as on determining the probability of reaching stability. All the theoretical findings will be illustrated in Section 4.

Steady states are the solutions of the random algebraic equation $\dot{p} = 0$, i.e. $rp(1 - pK) = cp$. Solving for p, we obtain two equilibrium points

$$p_1^* = 0, \quad p_2^* = \frac{(r-c)K}{r}. \tag{26}$$

Notice that, as previously indicated, if $c = 0$, $p_2^* = K$, that corresponds to the non-trivial equilibrium point for the classical logistic model.

We are interested in studying the linear stability of p_2^*. To this end, we introduce the variable $\hat{p}$ centred at that equilibrium value, $\hat{p}(t) = p(t) - p_2^*$. Then, the differential equation of model (2) can be written as

$$\hat{p}'(t) = r(\hat{p}(t) + p_2^*)\left(1 - \frac{1}{K}(\hat{p}(t) + p_2^*)\right) - c(\hat{p}(t) + p_2^*),$$

whose linearized form is

$$\hat{p}'(t) = \left(r - \frac{2r}{K}p_2^* - c\right)\hat{p}(t) + (r-c)p_2^* - \frac{r}{K}(p_2^*)^2.$$

In this manner, the original equation is written in the linearized form about the non-trivial equilibrium point, p_2^*, and it is known that if all the eigenvalues have negative real part, then the solution is linearly stable [40]. In our case this condition writes

$$r - \frac{2r}{K}p_2^* - c < 0 \Longleftrightarrow r - \frac{2r}{K}\frac{(r-c)K}{r} < c \Longleftrightarrow r\left(1 - \frac{2(r-c)}{r}\right) < c \Longleftrightarrow c < r.$$

Taking into account (26), this condition guarantees the non-trivial equilibrium state is positive, $p_2^* = \frac{(r-c)K}{r} > 0$. This fact admits an easy biological interpretation, namely, when the growth rate, r, is greater than the harvesting intensity determined by the coefficient c, the population does not tend to extinction but to $p_2^* > 0$. Observe that in our context both $r = r(\omega)$ and $c = c(\omega)$, $\omega \in \Omega$, are random variables, so the stability condition, $r(\omega) > c(\omega)$, happens with a certain probability, say π_s. Now, we compute this π_s under the general assumption that both random variables have an arbitrary joint p.d.f., $f_{r,c} := f_{r,c}(r, c)$ (which can be derived from the general setting by marginalizing with respect to p_0 and K the complete joint p.d.f., $f_{p_0,r,K,c)}$). To calculate π_s, we will apply the RVT technique. To this end, we first introduce the auxiliary random variable $Y(\omega) = r(\omega) - c(\omega)$, $\omega \in \Omega$, and define the following mapping

$$(r,\ c) \longmapsto (Y,\ Z) = (r - c,\ c)$$

whose inverse is

$$(Y,\ Z) \longmapsto (r,\ c) = (Y + Z,\ Z),$$

Observe that the Jacobian matrix determinant of the inverse mapping is 1. Then, according to the RVT method, the p.d.f. of random variable Y is

$$f_Y(y) = \int_{\mathcal{D}(Z)} f_{Y,Z}(y, z)\,\mathrm{d}z = \int_{\mathcal{D}(c)} f_{r,c}(y + c, c)\,\mathrm{d}c, \tag{27}$$

where $\mathcal{D}(Z)$ and $\mathcal{D}(c)$ represent the domains of the random variables $Z = Z(\omega)$ and $c = c(\omega)$, respectively. This function is useful to calculate probabilities of interest involving the random variable Y, in particular, we will use it to calculate π_s. Indeed, observe that the stability condition $r(\omega) > c(\omega)$ holds if and only if $Y(\omega) > 0$, $\omega \in \Omega$, so the probability of stability can be determined by

$$\pi_s = \mathbb{P}\left[\{\omega \in \Omega : Y(\omega) > 0\}\right] = \int_0^\infty f_Y(y)\,\mathrm{d}y = \int_0^\infty \int_{\mathcal{D}(c)} f_{r,c}(y + c, c)\,\mathrm{d}c\,\mathrm{d}y. \tag{28}$$

As in the numerical experiments that will be presented in the next section we will deal with the case that r and c are independent random variables, we now provide a more explicit expression for π_s. First, observe that in such a case (27) writes

$$f_Y(y) = \int_{\mathcal{D}(c)} f_r(y + c) f_c(c)\,\mathrm{d}c, \tag{29}$$

since $f_{r,c} = f_r f_c$. We now explicit the domain of integration in (29) in terms of the domains of random variables r and c, which is more useful in practice. Let $-\infty \le r_1 < r(\omega) < r_2 \le +\infty$ and $-\infty \le c_1 < c(\omega) < c_2 \le +\infty$ denote the domains of random variables r and c, respectively. The argument $y + c$ of the p.d.f. f_r appearing in the integral (29) must lie within the domain of random variable r. So, $r_1 - y < c < r_2 - y$ and expression (29) becomes

$$f_Y(y) = \int_{max(c_1,\, r_1 - y)}^{min(c_2,\, r_2 - y)} f_r(y + c) f_c(c)\,\mathrm{d}c.$$

Similarly, if we substitute this expression into (28) we can give sharper bounds for the domain of integration with respect to $Y(\omega)$ in terms of the explicit data that may be available in practice. Indeed, first observe that the domain of random variable Y is $r_1 - c_2 < Y(\omega) < r_2 - c_1$, $\omega \in \Omega$, so as there is no guarantee the difference $r_1 - c_2$ is positive, we impose $max(0,\ r_1 - c_2)$ as the lower integration limit. In this manner, taking into account (29), expression (28) writes

$$\pi_s = \int_{max(0,\, r_1 - c_2)}^{r_2 - c_1} f_Y(y)\,\mathrm{d}y = \int_{max(0,\, r_1 - c_2)}^{r_2 - c_1} \int_{max(c_1,\, r_1 - y)}^{min(c_2,\, r_2 - y)} f_r(y + c) f_c(c)\,\mathrm{d}c\,\mathrm{d}y. \tag{30}$$

Now we will obtain the 1-p.d.f. for the non-trivial equilibrium point, $p_2^* = \frac{(r-c)K}{r}$. To this end, we will apply the RVT method using the following mapping,

$$(r, K, c) \longmapsto (X, p_2^*, Z) = \left(r, \frac{(r-c)K}{r}, c\right). \tag{31}$$

It is easy to check that its inverse mapping is given by

$$(X, p_2^*, Z) \longmapsto (r, K, c) = \left(X, \frac{p_2^* X}{X-Z}, Z\right).$$

The Jacobian matrix determinant of the inverse mapping is

$$J(X, p_2^*, Z) = \det\left(\frac{\partial(r,K,c)}{\partial(X,p_2^*,Z)}\right) = \det\begin{pmatrix} \frac{\partial r}{\partial X} & \frac{\partial r}{\partial p_2^*} & \frac{\partial r}{\partial Z} \\ \frac{\partial K}{\partial X} & \frac{\partial K}{\partial p_2^*} & \frac{\partial K}{\partial Z} \\ \frac{\partial c}{\partial X} & \frac{\partial c}{\partial p_2^*} & \frac{\partial c}{\partial Z} \end{pmatrix} = \frac{r}{r-c} \neq 0.$$

So, using first the RVT method and secondly marginalizing with respect to r and c one obtains

$$f_{p_2^*}(p_2^*) = \int_{\mathcal{D}(r,c)} f_{r,K,c}\left(r, \frac{p_2^* r}{r-c}, c\right) \left|\frac{r}{r-c}\right| \mathrm{d}r\, \mathrm{d}c. \tag{32}$$

In the particular case that the random vector (r, c) is independent of the random variable K, the p.d.f. (32) of the equilibrium state can be expressed in terms of the following expectation

$$f_{p_2^*}(p_2^*) = \mathbb{E}_{r,c}\left[f_K\left(\frac{p_2^* r}{r-c}\right)\left|\frac{r}{r-c}\right|\right],$$

which is useful to compute the p.d.f. via Monte Carlo simulations.

Remark 4. Similarly as it has been explained in Remark 3, we can obtain the p.d.f. of the non-trivial equilibrium, p_2^*, considering alternative mappings to (31). Based on the motivation detailed in Remark 3, we may also use the following transformation

$$(r, K, c) \longmapsto (X, Y, p_2^*) = \left(r, K, \frac{(r-c)K}{r}\right). \tag{33}$$

Observe that the final expression that we would obtain using the mapping (33) is not the same as (32), but equivalent.

4. Numerical examples

The aim of this section is to illustrate, by means of two computational examples, the theoretical findings obtained in the previous section. To simplify the writing and facilitate the presentation in both examples, we will use the following terminology in agreement with the scenarios studied in Section 2

- Case I (Subsection 2.1): The capture is perpetually made from the time instant $t^{\mathrm{I}} = 1$.

- Case II (Subsection 2.2): The capture is made during the period $[t_1^{\mathrm{II}}, t_2^{\mathrm{II}}] = [1, 4]$.
- Case III (Subsection 2.3): A punctual capture is made at the time instant $t^{\mathrm{III}} = 1$.

In both examples, different parametric continuous probability distributions are assigned to inputs of the IVP (2). We will plot the 1-p.d.f. of the solution stochastic process, $f_{p(t)}$, as well as the p.d.f. of the equilibrium, $f_{p_2^*}$. We will graphically show convergence of $f_{p(t)}$ to $f_{p_2^*}$ as t increases, also determining the probability, π_s, of this convergence.

Example 1. *Let us consider model* (2) *and let us assume that all their input parameters are uniformly distributed as follows*

$$p_0 \sim U([0.22,\ 0.25]),\ \ r \sim U([0.13,\ 0.20]),\ \ K \sim U([0.4,\ 0.9]),\ \ c \sim U([0.09,\ 0.15]). \qquad (34)$$

Furthermore, we will also assume that p_0, r, K and c are independent random variables.

In Figure 1, we show the 1-p.d.f., $f_{p(t)}$, of the solution stochastic process of model (2) *at different time instants ($t \in \{5, 10\}$). In this graphical representation, we have considered the three types of captures analyzed in Subsections 2.1–2.3. These plots have been calculated by Monte Carlo with 25000 simulations using the expression* (11). *Comparing both graphical representations we can observe that, in Case I (when a perpetual capture is applied), the size of population reduces from $t = 5$ to $t = 10$, while in Cases II and III, the population increases because capture has been made before $t = 5$ (in Case II it is made during the period $t^{II} = [1, 4]$ and in Case III is punctually made at the time instant $t^{III} = 1$). These results are in full agreement with the biological interpretation. Finally, we observe that variability increases (i.e., uncertainty propagates) from $t = 5$ to $t = 10$ in the three scenarios.*

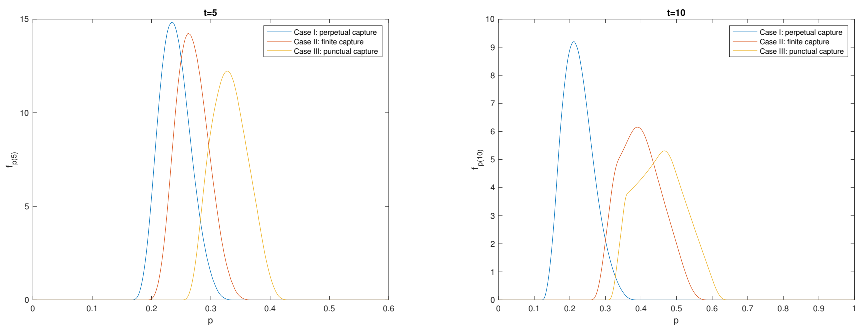

Figure 1: Approximation of the 1-p.d.f., $f_{p(t)}$, of the solution stochastic process of model (2) at $t = 5$ (left) and $t = 10$ (right) considering the three cases studied in Section 2. According to the description indicated at the beginning of this section, we have taken: $t^{\mathrm{I}} = 1$ (Case I), $[t_1^{\mathrm{II}}, t_2^{\mathrm{II}}] = [1, 4]$ (Case II) and $t^{\mathrm{III}} = 1$ (Case III). Example 1.

In Figure 2, we show the 1-p.d.f., $f_{p(t)}$, as a surface, i.e., its continuous evolution on the whole time interval $t \in [0, 5]$ in the three above-mentioned cases. On the surface, we have highlighted, by means of a solid line, the p.d.f. corresponding to the time instants $t^I = 1$ (Case I); $t_1^{II} = 1$ and $t_2^{II} = 4$ (Case II) and $t^{III} = 1$ (Case III). To facilitate the full view of these 3D-graphical representations, we recommend our readers to check the supplementary data, where subplots are shown separately in short video files from different views.

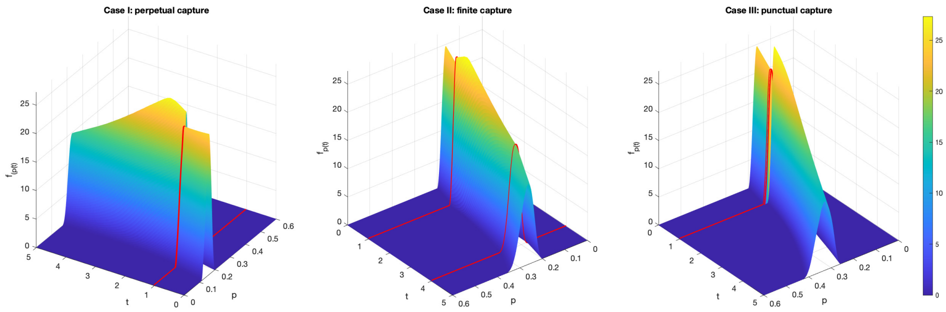

Figure 2: 3D-graphical representation of the 1-p.d.f., $f_{p(t)}$, for the time interval $t \in [0, 5]$ for the three cases studied in Section 2. Solid lines highlighted on each surface represent the corresponding p.d.f. at the time instants according to the description indicated at the beginning of this section: $t^{\mathrm{I}} = 1$ (Case I), $[t_1^{\mathrm{II}}, t_2^{\mathrm{II}}] = [1, 4]$ (Case II) and $t^{\mathrm{III}} = 1$ (Case III). A 360^o view is shown by a video in supplementary files. Example 1.

To illustrate the theoretical results about probabilistic stability analysis obtained in Section 3, we have represented the two scenarios indicated at the beginning of Section 3. In both scenarios, we have plotted the 1-p.d.f., $f_{p(t)}$, for different values of t and the p.d.f. of the equilibrium point, $f_{p_2^*}$, where p_2^* is given in (26)*. Specifically, we graphically show that $f_{p(t)}$ converges to $f_{p_2^*}$ as t increases. We have also calculated the probability of stability, π_s, using expression* (30)*. In Figure 3, we show these results when a perpetual capture (Case I) is applied. In this scenario, $\pi_s = 0.95$, so stability is reached with a high probability and it is clearly visualized in Figure 3.*

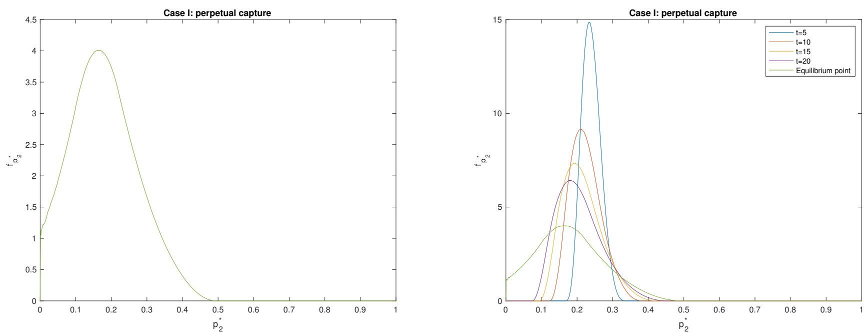

Figure 3: Left: P.d.f., $f_{p_2^*}$, of the equilibrium state p_2^* given in (26). Right: 1-p.d.f., $f_{p(t)}$, of the solution stochastic process for different values of $t \in \{5, 10, 15, 20\}$ together with $f_{p_2^*}$. Observe that the vertical scales in both plots are different to better visualize $f_{p_2^*}$ on the left panel. We can observe that $f_{p(t)}$ tends to $f_{p_2^*}$ as t increases. These plots correspond to Case I with $t^{\mathrm{I}} = 1$. Example 1.

As it has been explained in the previous section, for certain types of harvesting function that satisfy that $c(t; \omega) = 0$ for all $\omega \in \Omega$ as t is large enough, the equilibrium point matches the classical logistic model, i.e., the carrying capacity, that now is treated as a random variable $K = K(\omega)$. Cases II and III studied in Subsections 2.2 and 2.3, respectively, are examples of this particular scenario. In Figure 4, we illustrate these interesting cases. In both scenarios we can *see that the 1-p.d.f., $f_{p(t)}$ converges to the p.d.f., f_K of the carrying capacity, according to* (34)*, is a uniform distribution on the interval* [0.4, 0.9].

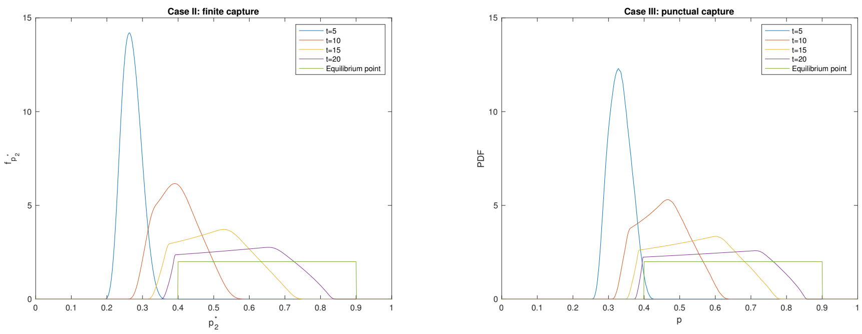

Figure 4: Plots of the 1-p.d.f., $f_{p(t)}$, of the solution stochastic process of model (2) at different fixed time instants and p.d.f. of the equilibrium point, $f_{p_2^*}$, when $p_2^* = K$ (carrying capacity). Left: Case II. Right: Case III. Example 1.

Example 2. *This second example is addressed to show that the theoretical results also correctly work when other probability distributions, different from the ones assumed in Example 1, are considered. For the sake of clarity, we follow a similar structure in the presentation. In this example, we will assume that each model input of the IVP* (2) *has truncated Beta distribution, $Be_{\mathcal{T}}(\alpha;\beta)$, where $\mathcal{T}$ denotes the truncation interval and $\alpha > 0$ and $\beta > 0$ are the so called shape parameters. It is important to point out that these distributions have been carefully chosen so that the corresponding values make biological sense (e.g., the distribution for p_0, which represents the initial population, has been chosen so that its values are smaller than the ones generated by the random variable K, that represents the carrying capacity). Specifically, we have taken*

$$\begin{aligned} r &\sim Be_{[0.4,0.6]}(5;1), & c &\sim Be_{[0.02,0.06]}(2;5), \\ p_0 &\sim Be_{[0.05,0.1]}(2;2), & K &\sim Be_{[0.8,1]}(3;4.5). \end{aligned}$$

Considering the above distributions, we perform a similar analysis as the one exhibited in the Example 1. In Figure 5, we have plotted the approximations of the 1-p.d.f., $f_{p(t)}$, at the time instants $t \in \{5, 10\}$ in the Case I (with $t^I = 1$), Case II ($[t_1^{II}, t_2^{II}] = [1, 4]$) and Case III ($t^{III} = 1$). Once again, it can be observed how greater values are expected for $p(t)$ in cases II and III. However, the increase (respect the values expected for case I) is smaller. Unlike in the uniform case, variability decreases for case II and case III in $t = 10$.

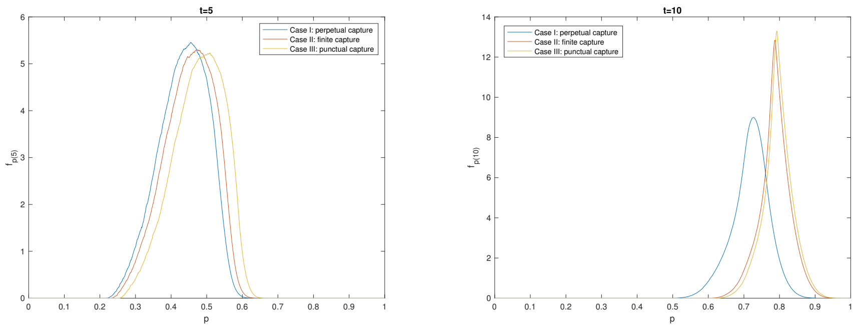

Figure 5: Approximation of the 1-p.d.f., $f_{p(t)}$, of the solution stochastic process of model (2) at $t = 5$ (left) and $t = 10$ (right) in the Case I (with $t^{\mathrm{I}} = 1$), Case II ($[t_1^{\mathrm{II}}, t_2^{\mathrm{II}}] = [1, 4]$) and Case III ($t^{\mathrm{III}} = 1$). Example 2.

In Figure 6, we show 3-D graphical representations corresponding to the 1-p.d.f.'s, $f_{p(t)}$, represented in Figure 5. On the surface, we have highlighted, by means of a solid line, the p.d.f. corresponding to the time instants $t^I = 1$ (Case I); $t_1^{II} = 1$ and $t_2^{II} = 4$ (Case II) and $t^{III} = 1$ (Case III). Once again, we encourage readers to see video files added as supplementary data to better visualize the plots.

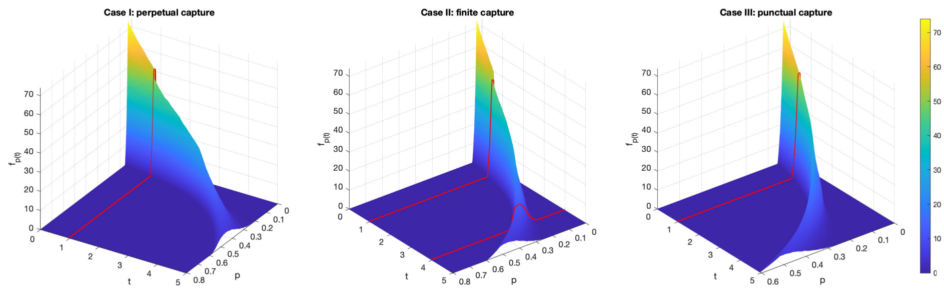

Figure 6: 3D-graphical representation of the 1-p.d.f., $f_{p(t)}(p)$, for the time interval $t \in [0, 5]$ for the three cases studied in Section 2. On the surface, we have highlighted, by means of a solid line, the p.d.f. corresponding to the time instants $t^{\mathrm{I}} = 1$ (Case I); $t_1^{\mathrm{II}} = 1$ and $t_2^{\mathrm{II}} = 4$ (Case II), and $t^{\mathrm{III}} = 1$ (Case III). A 360^o view is shown by a video in supplementary files. Example 2.

As in the Example 2, in Figure 7, we have represented the p.d.f., $f^*_{p_2}$, of the equilibrium random variable, p_2^*, given in (26) (left panel) and the convergence of the 1-p.d.f.'s, $f_{p(t)}$, towards $f^*_{p_2}$ in Case I (right panel). In this case, the probability of stability is even higher, with a value of $\pi_s = 0.9994$. The particular case that the equilibrium is just the carrying capacity, i.e. $p_2^* = K$, is shown in Figure 8. The Case II is shown on the left panel while the Case III is represented on the right panel.

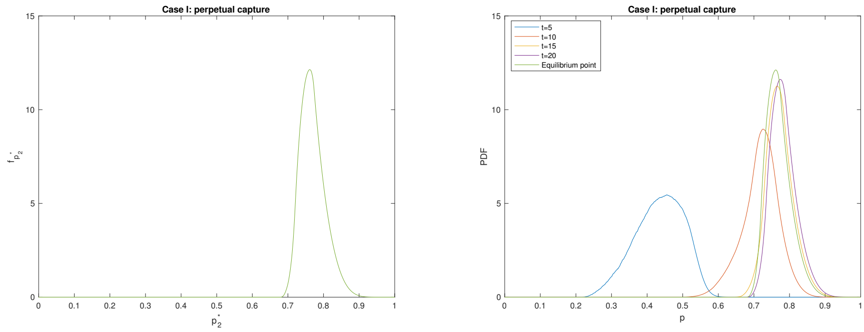

Figure 7: Left: P.d.f. of the equilibrium random variable, p_2^*, given in (26). Right: Convergence of the 1-p.d.f.'s, $f_{p(t)}$, towards $f^*_{p_2}$ in the Case I with $t^{\mathrm{I}} = 1$. Example 2.

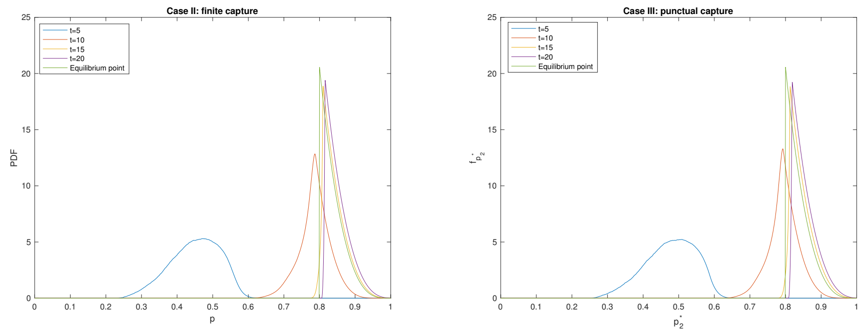

Figure 8: Convergence of the 1-p.d.f.'s, $f_{p(t)}$, towards the p.d.f. $f^*_{p_2}$, in the case that the equilibrium random variable is the carrying capacity, $p_2^* = K$. Left: Case II with $t_1^{\mathrm{II}} = 1$ and $t_2^{\mathrm{II}} = 4$. Right: Case III with $t^{\mathrm{III}} = 1$. Example 2.

5. Application to real-world data

The objective of this section is to show how we can take advantage of the theoretical results established throughout the paper when real-world data are available. Specifically, we shall show how to reasonably determine the probability distributions of the model inputs of the randomized hybrid logistic model (2), that considers different stochastic processes with jump as harvesting functions in its formulation. The stochastic calibration process will be thoroughly described so that it is easily reproducible by interested readers.

Fisheries policies are responsible for setting fishing quotes and limits in their respective countries, looking for the maintenance of species' stock as well as to increase (or at least keep) humans' employment rate and food resources. Governments' decisions need to be made with the objective of minimising the probability of disastrous scenarios, such as stock collapse. In other words, policies need to ensure relatively high benefits with low risk. Stock assessment methods use collected data to describe, by means of mathematical models, hypothetical situations that can help decision makers with their resolution. In this section, we are going to probabilistically describe the dynamics of fish population via the randomized model (2) that considers not only species' growth rate but also the carrying capacity of the environment and temporary capture periods. The study takes into account uncertainties coming from both the inherent complexity of the problem and sampled data. We will use data corresponding to the stock of Beaked Redfish in the Barents Sea from 1992 to 2018 [41]. For convenience with the mathematical notation introduced in the IVP (2), we identify $t_0 = 1992$, so $t_{26} = 2018$. Hereinafter, sampled data at every time instant t_i, $i = 0, 1, \ldots, 26$, will be denoted by p_i. These values are plotted in Figure 9.

Based on these monitored data, we have assumed that captures are made from 2005 to 2008. This corresponds to Case II studied in Subsection 2.2 and with the notation introduced at the beginning of Section 4, we take $t_1^{\mathrm{II}} = 2005$ and $t_2^{\mathrm{II}} = 2008$. We will assume that model parameters, p_0, r, K and c are independent random variables whose distributions will be specified later. The calibration process consists of three main steps. First, we will assign flexible parametric distributions according to the biological interpretation of each one of them. Secondly, we will perform a deterministic fitting that allows us to take plausible initial parameters of the distributions assumed to each model input. Finally, an optimisation algorithm will be implemented to determine the best values of the parameters of the input distributions by minimizing a certain error. Several techniques can be used when calibrating models, however, we have chosen this particular technique since it has been successfully used by some of the authors recently in [42] with promising results within the setting of another stochastic model.

Regarding input parameters in the IVP (2), there is not much information. All parameters are assumed to be positive, since negative values are not coherent with their biological meaning. Moreover, the random variable $p_0 = p_0(\omega)$, that represents the population stock at the initial time instant, $t_0 = 1992$, is assumed to vary in a domain whose greatest value is bounded by the lowest value of the carrying capacity, $K = K(\omega)$, which, in turn, has been assumed to be bounded by a fraction of 120% of the maximum stock value, i.e $1.277 \times 1,20 = 1.5324$. The growing rate, $r = r(\omega)$, and the capture intensity, $c = c(\omega)$, are random variables whose, respective domains, have been limited too. Firstly, the upper end of the domain of c has been assumed to be smaller than lower end of the domain of r (otherwise there would be a chance that population will decrease over time, a feature that is not observed in sampled data, see Figure 9). Finally, the lower end of the domain of random variable r is limited to values larger than 0.005, in order to avoid dividing by 0. Taking into account these intuitive constraints, we will assume that p_0 and K have uniform distributions, i.e. $p_0 \sim \mathrm{U}(p_{0,1},\ p_{0,2})$ and $K \sim \mathrm{U}(k_1,\ k_2)$ such that $p_{0,2} < k_1$ and $k_2 < 1.5324$. Since random variable r is positive, we will assume that it has a truncated Gamma distribution with parameters $r_1 > 0$ and $r_2 > 0$, i.e. $r \sim \mathrm{Ga}|_{\mathcal{T}_r}(r_1; r_2)$, where the domain of truncation is $\mathcal{T}_r = (t_{r,1}, t_{r,2})$; here we take $t_{r,1} = 0.005$ and $t_{r,2} = \infty$. For random variable c, which is also positive, we will assume that follows a truncated Gaussian distribution with parameters μ_c and $\sigma_c > 0$, i.e. $c \sim N|_{\mathcal{T}_c}(\mu_c; \sigma_c)$, where $\mathcal{T}_c = (t_{c,1}, t_{c,2})$, $t_{c,1} > 0$. Our objective is to obtain appropriate values for these parameters so that the response of model (2) captures the variability of the sampled data. For each $t = t_n$, $n = 1, 2, \ldots, 26$, the response will be constructed by means of the expectation, $\mu_p(t) := \mathbb{E}[p(t)]$, and the variance, $\sigma_p^2(t) := \mathbb{V}[p(t)]$, which can be calculated

$$\mu_p(t) = \int_{-\infty}^{\infty} p f_{p(t)}(p)\,\mathrm{d}p, \quad \sigma_p^2(t) = \int_{-\infty}^{\infty} (p - \mu_p(t))^2 f_{p(t)}(p)\,\mathrm{d}p, \tag{35}$$

where $f_{p(t)}$ is given in (9). From these two moments, at every time instant $t = t_n$, we will construct confidence intervals at certain prefixed confidence level, $1-\alpha$, $\alpha \in]0,1[$,

$$\begin{aligned} 1-\alpha &= \mathbb{P}\left[\left\{\omega \in \Omega : p(t)(\omega) \in [\mu_p(t) - \nu_t \sigma_p(t), \mu_p(t) + \nu_t \sigma_p(t)]\right\}\right] \\ &= \int_{\mu_p(t)-\nu_t\sigma_p(t)}^{\mu_p(t)+\nu_t\sigma_p(t)} f_{p(t)}(p)\, \mathrm{d}p. \end{aligned}$$

Here, ν_t represents the radius of the confidence interval which varies with t. This is advantageous since we dynamically construct the confidence interval to the specific requirements according to the prefixed level of confidence, instead of using classical approximations where this radius is a common constant for all the time instants, t. One typically takes $\nu_t = 1.96 \approx 2$, which corresponds to the Gaussian approximation.

As previously indicated, as a first approximation we will perform a deterministic calibration of model inputs, p_0, r, K and c. To this end, we use the command *NonlinearModelFit* in the software Mathematica® [43]. It gives approximate values of model inputs and their corresponding associated errors. The obtained values are

$$\begin{array}{rclcrcl} \tilde{p}_0 &=& 0.53003, & & \epsilon_{p_0} &=& 0.017537, \\ \tilde{r} &=& 0.109922, & & \epsilon_r &=& 0.0124091, \\ \tilde{c} &=& 0.0823592, & & \epsilon_c &=& 0.0102977, \\ \tilde{K} &=& 1.53234, & & \epsilon_K &=& 0.103674. \end{array}$$

These values are interpreted as suitable references for the mean and the variance of the model inputs of the randomized IVP (2). Next, we will take them as starting values when the optimisation algorithm will be applied to determine the best values of parameters k_1, k_2 $p_{0,1}$, $p_{0,2}$, r_1, r_2, μ_c, σ_c, $t_{c,1}$ and $t_{c,2}$. Before performing this final calibration, we will reduce the number of parameters to be determined by estimating $t_{c,1}$ and $t_{c,2}$, i.e. the truncation interval $\mathcal{T}_c = (t_{c,1}, t_{c,2})$ of Gaussian random variable c. This is done by considering that $c \sim \mathrm{N}|_{\mathcal{T}_c}(c; \epsilon_c) = \mathrm{N}|_{\mathcal{T}_c}(0.0823592; 0.0102977)$, where $\mathcal{T}_c = (0.02, 0.2)$, since one verifies

$$\int_{0.02}^{0.2} \frac{1}{\sqrt{2 \times \pi \times 0.0102977}} \exp\left[-\frac{1}{2}\left(\frac{c - 0.0823592}{0.0102977}\right)^2\right] \mathrm{d}c \approx 1.$$

Notice that the choice of the domain of integration is also supported by the Bienaymé–Chebyshev inequality [35].

To obtain the initial estimates, that will be taken later as seeds or starting values when applying the optimization algorithm, for rest of parameters on which the probability distributions assigned to model inputs depend on, we will apply the Moment Matching Method [35]. By denoting these unknown values as $\{p_{0,1}^{(0)}, p_{0,2}^{(0)}\}$, $\{r_1^{(0)}, r_2^{(0)}\}$ and $\{k_1^{(0)}, k_2^{(0)}\}$, and using the respective distribution formulas for mean and variance (moments), one obtains the following nonlinear systems,

$$\begin{array}{rclcrcl} \mathbb{E}[p_0] &=& \frac{p_{0,1}^{(0)} + p_{0,2}^{(0)}}{2} = 0.53003, & & \mathbb{V}[p_0] &=& \frac{\left(p_{0,1}^{(0)} - p_{0,2}^{(0)}\right)^2}{12} = 0.017537, \\ \mathbb{E}[r] &=& \frac{r_1^{(0)}}{r_2^{(0)}} = 0.109922, & & \mathbb{V}[r] &=& \frac{r_1^{(0)}}{\left(r_2^{(0)}\right)^2} = 0.0124091, \\ \mathbb{E}[K] &=& \frac{k_1^{(0)} + k_2^{(0)}}{2} = 1.53234, & & \mathbb{V}[K] &=& \frac{\left(k_1^{(0)} - k_2^{(0)}\right)^2}{12} = 0.103674. \end{array}$$

Solving the three independent systems with the command *FindRoot* of Mathematica® software, yields

$$p_{0,1}^{(0)} = 0.499655, \qquad p_{0,2}^{(0)} = 0.56040,$$

$$r_1^{(0)} = 78.467, \qquad r_2^{(0)} = 0.00140086,$$

$$k_1^{(0)} = 1.35277, \qquad k_2^{(0)} = 1.71191.$$

Denoting $\boldsymbol{\xi} = (p_{0,1}, p_{0,2}, r_1, r_2, k_1, k_2, \mu_c, \sigma_c)$ to simplify the notation, we finally define the error function, $E = E(\boldsymbol{\xi})$, to be minimized as the sum of the squared differences between the expectation $\mu_p(t_i; \boldsymbol{\xi}) = \mathbb{E}[p(t_i; \boldsymbol{\xi})]$ of the solution stochastic process evaluated at every time instant of the sample, t_i, $i = 0, 1, \ldots, 26$, and the corresponding sampled data p_i,

$$E = E(\boldsymbol{\xi}) = \sum_{i=0}^{26} (\mu_p(t_i; \boldsymbol{\xi}) - p_i)^2. \tag{36}$$

Notice that $\mu_p(t_i; \boldsymbol{\xi})$ can be calculated via the 1-p.d.f., $f_{p(t)}$, using the expression (35). We have used the command *NMinimize* function from Mathematica® software to minimize the error function (36) imposing the aforementioned restrictions $p_{0,2} < k_1$, $k_2 < 1.5324$, $0 < p_{0,1} < p_{0,2}$ and $0 < k_1 < k_2$. This yields the optimal values of the parameters of the probability distributions assigned to model inputs

$$p_{0,1} = 0.493908, \quad p_{0,2} = 0.567161,$$

$$r_1 = 70.0067, \qquad r_2 = 0.00155884,$$

$$k_1 = 1.33852, \qquad k_2 = 1.76292,$$

$$\mu_c = 0.0824084, \quad \sigma_c = 0.0107208.$$

Therefore, summarizing,

$$\begin{aligned} p_0 &\sim \mathrm{U}\,(0.493908, 0.567161)\,, \quad & r &\sim \mathrm{Ga}|_{(0.005,\infty)}\,(70.0067; 0.00155884)\,, \\ K &\sim \mathrm{U}\,(1.33852, 1.76292)\,, \quad & c &\sim \mathrm{N}|_{(0.02,0.2)}\,(0.0824084; 0.0107208)\,. \end{aligned} \tag{37}$$

In order to properly evaluate the quality of the calibration, in Figure 9, we have represented the expectation of the solution stochastic process, $\mu_{p(t)}$, the confidence interval $\mu_{p(t)} \pm 1.75\sigma_{p(t)}$ and the sampled data. The confidence interval has been calculated using expressions (35) and (5), with $\alpha = 0.1$, and taking as $1.75 = \nu_t = \max \nu_{t_i} : i = 0, 1, \ldots, 26$ in order to guarantee, at least, 90%-confidence intervals at every time instant t_i. The involved integrals have been approximated using the command *NIntegrate* in Mathematica® software. In Figure 9, we can see that our probabilistic calibration is able to capture uncertainties in the dynamics of sampled data.
To complete our probabilistic analysis, in Figure 10, we show the evolution of the estimate 1-p.d.f., $p(t)$, of the stock of Beaked Redfish in the Barents Sea during the period 1992 – 2018 by a 3D-plot. For the sake of clarity, we have also included in the plot the result shown in Figure 9. It can be observed how values of p tend to a certain mean value with a variability, that has been modelled by the random variable K, according to the distribution given in (37).

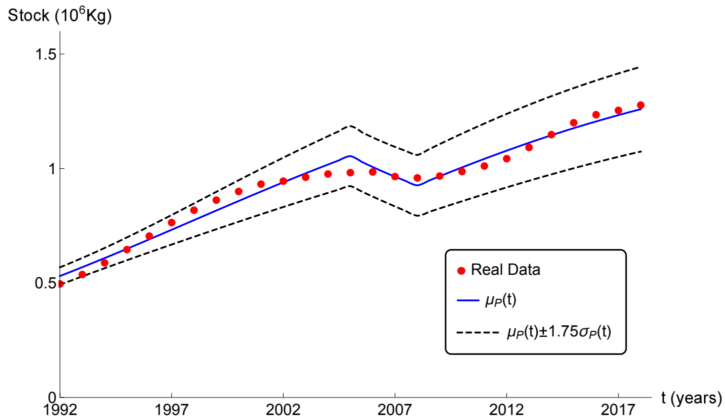

Figure 9: Probabilistic fitting (mean and 92%-confidence intervals) of sampled data corresponding to stock of Beaked Redfish in the Barents Sea during the period 1992 – 2018 [41] using the 1-p.d.f., $f_{p(t)}$, of the solution stochastic process given in (9) of the randomized hybrid logistic model (2) with captures made during the period 2005 – 2008. This scenario corresponds to Case II described in Subsection 2.2.

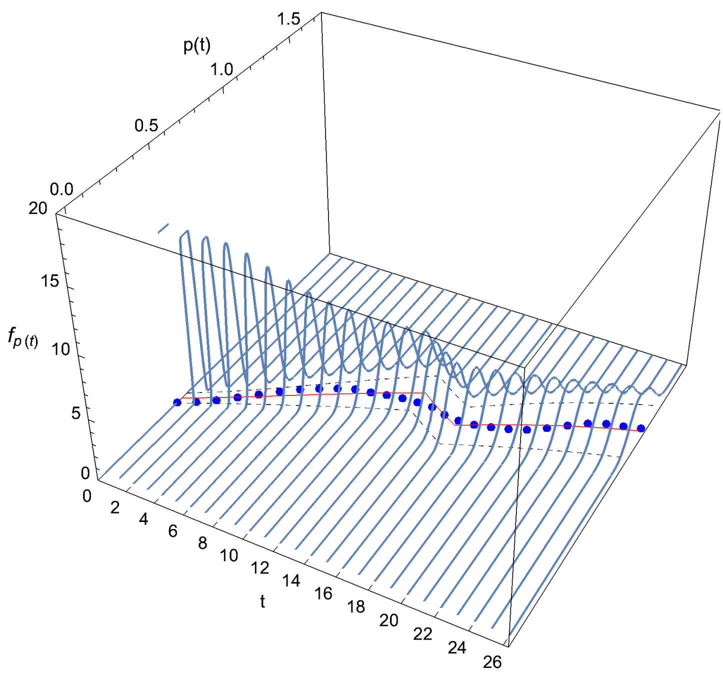

Figure 10: Evolution of the 1-p.d.f., $f_{p(t)}$, over the period 1992 – 2018 together with the mean and 92%-confidence intervals plotted in Figure 9.

The above-described calibration process has been summarized in the next image.

Inputs

- Time instants: $t_i,\ i = 0, 1, \ldots, N$.
- Population stock at t_i: $p_i,\ i = 0, 1, \ldots, N$.
- Time instants when captures were performed, $t_1^j,\ t_2^j,\ j \in \{I, II, III\}$.

Step 1: Assignment of random parametric distributions to model parameters

$$p_0 \sim \mathrm{U}\left(p_{0,1}, p_{0,2}\right), \qquad r \sim \mathrm{Ga}|_{\mathcal{T}_r}\left(r_1; r_2\right),$$

$$K \sim \mathrm{U}\left(k_1, k_2\right), \qquad c \sim \mathrm{N}|_{\mathcal{T}_c}\left(\mu_c; \sigma_c\right).$$

Step 2: Deterministic calibration of model parameters

NonLinearModelFit()

Obtention of the values $\tilde{p_0}, \tilde{r}, \tilde{K}, \tilde{c}, \epsilon_{p_0}, \epsilon_r, \epsilon_K, \epsilon_c$.

Step 3: Obtention of the truncation intervals

$$\mathcal{T}_c = [t_{c,1}, t_{c,2}] \text{ such that } t_{c,1} > 0 \text{ and } \int_{t_{c,1}}^{t_{c,2}} f_c(c)\mathrm{d}c = 1,$$

$$\mathcal{T}_r = [t_{r,1}, t_{r,2}] \text{ such that } t_{r,1} > 0 \text{ and } \int_{t_{r,1}}^{t_{r,2}} f_r(r)\mathrm{d}r = 1,$$

where f_c and f_r are the PDF of c and r, respectively.

Step 4: Computation of the initial values of the parameters distribution

(Matching Moments Method)

Determine $p_{0,1}^{(0)}, p_{0,2}^{(0)}, r_1^{(0)}, r_2^{(0)}, k_1^{(0)}, k_2^{(0)}, \mu_c^{(0)}$ and $\sigma_c^{(0)}$ such that

$$\tilde{p_0} = \mathbb{E}[p_0] = \frac{p_{0,1}^{(0)} + p_{0,2}^{(0)}}{2}, \qquad \epsilon_{p_0} = \mathbb{V}[p_0] = \frac{\left(p_{0,1}^{(0)} - p_{0,2}^{(0)}\right)^2}{12},$$

$$\tilde{r} = \mathbb{E}[r] = \frac{r_1^{(0)}}{r_2^{(0)}}, \qquad \epsilon_r = \mathbb{V}[r] = \frac{r_1^{(0)}}{\left(r_2^{(0)}\right)^2},$$

$$\tilde{K} = \mathbb{E}[K] = \frac{k_1^{(0)} + k_2^{(0)}}{2}, \qquad \epsilon_K = \mathbb{V}[K] = \frac{\left(k_1^{(0)} - k_2^{(0)}\right)^2}{12},$$

$$\tilde{c} = \mathbb{E}[c] = \mu_c^{(0)}, \qquad \epsilon_c = \mathbb{V}[c] = \sigma_c^{(0)}.$$

Check that the obtained results make sense (e.g., $p_{0,2} < k_1$).

Step 5: Definition of the error function

$$E = E(\boldsymbol{\xi}) = \sum_{i=0}^{N} (\mu_p(t_i; \boldsymbol{\xi}) - p_i)^2,$$

where $\boldsymbol{\xi} = (p_{0,1}, p_{0,2}, r_1, r_2, k_1, k_2, \mu_c, \sigma_c)$ and μ_p is defined in expression (35).

Step 6: Minimization of the error function

NMinimize()

Results obtained in Step 4 are used as starting points.

Step 7: Computation of the expectation and confidence interval of the solution

- Computation of $f_{p(t)}(p)$ using equation (10), with $q(z)$ and $h(t)$ defined in (3) (4), respectively.
- Computation of the expectation and the variance using equation (35).
- Calculation of the confidence interval. Set $\alpha \in [0, 1]$ such that $1 - \alpha$ represents the prefixed confidence level. Seek ν_t values such that

$$\int_{\mu_p(t) - \nu_t \sigma_p(t)}^{\mu_p(t) + \nu_t \sigma_p(t)} f_{p(t)}(p)\,\mathrm{d}p \geq 1 - \alpha, \quad \alpha \in [0, 1].$$

End

Figure 11: Flowchart algorithm corresponding to the probabilistic calibration in the context of the real-world application presented in Section 5. In the application we have taken $N = 26$ and $j = II$ with $t_1^{\mathrm{II}} = 2005$ and $t_2^{\mathrm{II}} = 2008$.

6. Conclusions

In this paper we have performed a full probabilistic analysis of the randomized logistic model with an influence term that describes captures or harvesting, via different functional forms represented by discontinuous stochastic processes. We have taken extensive advantage of the so called Random Variable Transformation to conduct our study, which has been based on obtaining the first probability density function of the solution stochastic process of the aforementioned hybrid randomized logistic model. The obtained results are, from a probabilistic standpoint very general, since we assume abstract joint densities for all the model inputs. We have illustrated our theoretical findings by means of two numerical examples where different distributions are assumed for model inputs. To complete our contribution, we have carefully detailed, how our theoretical results can be applied in practice when real data are available. This application has been described so that it can be fully reproducible for anyone interested in it. At this point, it is interesting to underline that in the setting of the real-world application shown in the paper, the choice of the probability distributions for each one of the model parameters has been done on the basis of plausible distributions according to the biological interpretation of model parameters as positiveness, boundedness, etc., however it would be desirable to find out optimal methods that do not limit the applications of our theoretical results, which rely on the fact that the probability distributions of the model parameters are know. This is an open challenge for the Uncertainty Quantification community that we will continue facing in our future research. To the best of our knowledge, this is the first time that a hybrid random differential equation (i.e., a random differential equation having discontinuous stochastic processes in its formulation) is studied by computing the first probability density of its solution via the Random Variable Transformation method. In this sense, we think the ideas exhibited throughout the paper could be useful to open new avenues in the area of random differential equations. In particular, in our prospective work, we plan to apply the probabilistic analysis performed in this paper to other relevant models whose right hand side is discontinuous. We also bear in mind the possibility of conveniently reinterpret the model in the setting of stochastic control to design stable controler so that specific biological targets are met. In this manner, we hope to continue helping to extent deterministic theory to the random setting using the approach based on Random Differential Equations.

Acknowledgements

This work has been partially supported by the grant PID2020-115270GB–I00 funded by MCIN/AEI/10.13039/501100011033 and the grant AICO/2021/302 (Generalitat Valenciana).

Conflict of Interest Statement

The authors declare that there is no conflict of interests regarding the publication of this article.

[1] T. Malthus, An Essay on the Principle of Population and Other Writings, Penguin Classics, London, 1798.

[2] M. Efendiev, Evolution Equations Arising in the Modelling of Life Sciences, 1st Edition, Vol. 163 of International Series of Numerical Mathematics, Birkhuser Basel, 2013.

[3] D. Fischer, The Great Wave: Price Revolutions and the Rhythm of History, Oxford University Press, New York, 1996.

[4] S. Jørgensen, B. Fath, S. Bastianoni, J. Marques, F. Muller, S. Nielsen, B. Patten, E. Tiezzi, R. Ulanowicz, A New Ecology: Systems Perspective, Elsevier, The Netherlands, 2007.

[5] S. Jørgensen, B. Fath, Fundamentals of Ecological Modelling, Vol. 23 of Developments in Environmental Modelling, Elsevier, The Netherlands, 2011.

[6] D. Stanescu, B. Chen-Charpentier, B. J. Jensen, P. J. Colberg, Random coefficient differential models of growth of anaerobic phtotsyntetic bacteria, Electronic Transactions on Numerical Analysis 34 (2008) 44–58.

[7] D. Xiu, G. Karniadakis, The Wiener–Askey Polynomial Chaos for Stochastic Differential Equations, Journal on Scientific Computing 24 (2002) 619–644. doi:10.1137/S1064827501387826.

[8] C. Braumann, Growth and extinction of populations in randomly varying environments, Computers & Mathematics with Applications 56 (3) (2008) 631–644. doi:https://doi.org/10.1016/j.camwa.2008.01.006.

[9] G. Jumarie, New stochastic fractional models for Malthusian growth, the Poissonian birth process and optimal management of populations, Mathematical and Computer Modelling 44 (3) (2006) 231–254. doi:https://doi.org/10.1016/j.mcm.2005.10.003.

[10] J. Cortés, L. Jódar, L. Villafuerte, Random linear-quadratic mathematical models: Computing explicit solutions and applications, Mathematics and Computers in Simulation 79 (7) (2009) 2076–2090. doi:https://doi.org/10.1016/j.matcom.2008.11.008.

[11] P. F. Verhulst, Notice sur la loi que la population poursuit dans son accroisse-ment, in: Correspondance mathematique et physique, Vol. 10, Ghent, 1838, pp. 113–121.

[12] R. Pearl, L. Reed, On the Rate of Growth of the Population of the United States since 1790 and Its Mathematical Representation 6 (6) (1920) 275–288. doi:10.1073/pnas.6.6.275.

[13] H. Safuan, Z. Jovanoski, I. Towers, H. Sidhu, Exact solution of a non-autonomous logistic population model, Ecological Modelling 251 (2013) 99–102. doi:https://doi.org/10.1016/j.ecolmodel.2012.12.016.

[14] V. Yukalov, E. Yukalova, D. Sornette, Punctuated evolution due to delayed carrying capacity, Physica D: Nonlinear Phenomena 238 (2009) 1752–1767. doi:https://doi.org/10.1016/j.physd.2009.05.011.

[15] P. MiÅkinis, V. Vasiliauskien, The analytical solutions of the harvesting Verhulsts evolution equation, Ecological Modelling 360 (2017) 189–193. doi:https://doi.org/10.1016/j.ecolmodel.2017.06.021.

[16] B. Øksendal, Stochastic Differential Equations, second edition Edition, Springer-Verlag, Berlin, 1980. doi:https://doi.org/10.1007/978-3-662-02574-1.

[17] P. Kloeden, E. Platen, Numerical Solution of Stochastic Differential Equations, Vol. 23 of Applications of Mathematics, Springer-Verlag, Berlin, 1999. doi:https://doi.org/10.1007/978-3-662-12616-5.

[18] E. Allen, Modeling with Itô Stochastic Differential Equations, Mathematical Modelling: Theory and Applications, Springer Netherlands, 2007. doi:https://doi.org/10.1007/978-1-4020-5953-7.

[19] J. Golec, S. Sathananthan, Stability analysis of a stochastic logistic model, Mathematical and Computer Modelling 38 (2003) 585–593. doi:https://doi.org/10.1016/S0895-7177(03)90029-X.

[20] X. Sun, Y. Wang, Stability analysis of a stochastic logistic model with nonlinear diffusion term, Applied Mathematical Modelling 32 (2008) 2067–2075. doi:https://doi.org/10.1016/j.apm.2007.07.012.

[21] P. Kink, Some analysis of a stochastic logistic growth model, Stochastic Analysis and Applications 36 (2018) 240–256. doi:10.1080/07362994.2017.1393343.

[22] H. Schurz, Modeling, analysis and discretization of stochastic logistic equations, International Journal of Numerical Analysis and Modeling 4 (2) (2007) 178–197.

[23] O. Otunuga, Time-dependent probability density function for general stochastic logistic population model with harvesting effort, Physica A: Statistical Mechanics and its Applications 573. doi:https://doi.org/10.1016/j.physa.2021.125931.

[24] M. Liu, K. Wang, Q. Hong, Stability of a stochastic logistic model with distributed delay, Mathematical and Computer Modelling 57 (2013) 1112–1121. doi:https://doi.org/10.1016/j.mcm.2012.10.006.

[25] M. Liu, D. Fan, K. Wang, Stability analysis of a stochastic logistic model with infinite delay, Communications in Nonlinear Science and Numerical Simulation 18 (2013) 2289–2294. doi:https://doi.org/10.1016/j.cnsns.2012.12.011.

[26] L. Sun, H. Zhu, Y. Ding, Impulsive control for persistence and periodicity of logistic systems, Mathematics and Computers in Simulation 171 (2020) 294–305. doi:https://doi.org/10.1016/j.matcom.2019.06.006.

[27] H. Yoshioka, A simplified stochastic optimization model for logistic dynamics with control-dependent carrying capacity, Journal of Biological Dynamics 13 (2019) 148–176. doi:10.1080/17513758.2019.1576927.

[28] T. Soong, Random Differential Equations in Science and Engineering, Vol. 103 of Mathematics in Science and Engineering, Academic Press, New York, 1973.

[29] R. Smith, Uncertainty Quantification: Theory, Implementation, and Applications, Computational Science and Engineering, Society for Industrial and Applied Mathematics, Philadelphia, 2014.

[30] F. Dorini, M. Cecconello, L. Dorini, On the logistic equation subject to uncertainties in the environmental carrying capacity and initial population density, Communications in Nonlinear Science and Numerical Simulation 33 (2016) 160–173. doi:https://doi.org/10.1016/j.cnsns.2015.09.009.

[31] F. Dorini, N. Bobko, L. Dorini, A note on the logistic equation subject to uncertainties in parameters, Computational and Applied Mathematics 37 (2018) 1496–1506. doi:10.1007/s40314-016-0409-6.

[32] J. Calatayud, J.-C. Corts, F. A. Dorini, M. Jornet, On a stochastic logistic population model with time-varying carrying capacity, Computational and Applied Mathematics 39. doi:10.1007/s40314-020-01343-z.
[33] J. Calatayud, J.-C. Corts, F. Dorini, On the Random Non-Autonomous Logistic Equation with Time-Dependent Coefficients, Fluctuation and Noise Lettersdoi:https://doi.org/10.1142/S0219477521500383.
[34] T. Neckel, F. Rupp, Random Differential Equations in Scientific Computing, Walter De Gruyter, Berlin, 2013.
[35] G. Casella, R. Berge, Statistical inference, 2nd Edition, Duxbury advanced series, Duxbury Thomson Learning, Pacific Grove, 2002.
[36] M.-C. Casabn, J.-C. Corts, A. Navarro-Quiles, J.-V. Romero, M.-D. Rosell, R.-J. Villanueva, A comprehensive probabilistic solution of random SIS-type epidemiological models using the random variable transformation technique, Communications in Nonlinear Science and Numerical Simulation 32 (2016) 199–210. doi:https://doi.org/10.1016/j.cnsns.2015.08.009.
[37] D. Kroese, T. Taimre, Z. Botev, Handbook of Monte Carlo Methods, Vol. 706 of Wiley Series in Probability and Statistics, Wiley, 2013.
[38] D. Baowan, B. Cox, T. Hilder, J. Hill, N. Thamwattana, Chapter 2 - mathematical preliminaries, in: D. Baowan, B. J. Cox, T. A. Hilder, J. M. Hill, N. Thamwattana (Eds.), Modelling and Mechanics of Carbon-Based Nanostructured Materials, Micro and Nano Technologies, William Andrew Publishing, 2017, pp. 35–58. doi:https://doi.org/10.1016/B978-0-12-812463-5.00002-9.
[39] R. Hoskins, Delta Functions: Introduction to Generalised Functions, 2nd Edition, Elsevier Science, 2009.
[40] P. Glendinning, D. Crighton, M. Ablowitz, S. Davis, E. Hinch, A. Iserles, J. Ockendon, P. Olver, Stability, Instability and Chaos: An Introduction to the Theory of Nonlinear Differential Equations, Cambridge Texts in Applied Mathematics, Cambridge University Press, Cambridge, 1994.
[41] Environmental monitoring of svalbard and jan mayen norsk search all of mosj, `https://www.mosj.no/en/fauna/marine/deep-sea-redfish.html`.
[42] V. Bevia, C. Burgos, J.-C. Corts, A. Navarro-Quiles, R.-J. Villanueva, Uncertainty quantification analysis of the biological gompertz model subject to random fluctuations in all its parameters, Chaos, Solitons & Fractals 138 (2020) 109908. doi:https://doi.org/10.1016/j.chaos.2020.109908.
[43] I. Wolfram Research, Mathematica, Version 12.2, champaign, IL, 2020.
URL `https://www.wolfram.com/mathematica`